Acta Crystallographica Section B
Structural Science
ISSN 0108-7681

(3 + 1)-Dimensional structure refinement of the fresnoite framework-structure type compound $Ba_2TiGe_2O_8$

Thomas Höche,[a]*† Saeid Esmaeilzadeh,[b] Reinhard Uecker,[c] Sven Lidin[b] and Wolfgang Neumann[a]

[a]AG Kristallographie, Institut für Physik, Humboldt-Universität zu Berlin, Invalidenstrasse 110, D-10115 Berlin, Germany, [b]Department of Inorganic Chemistry, Arrhenius Laboratory, Stockholm University, S-106 91 Stockholm, Sweden, and [c]Institut für Kristallzüchtung im Forschungsverbund Berlin e.V., Max-Born-Straße 2, D-12489 Berlin, Germany

† Current address: Institut für Oberflächenmodifizierung e.V., Permoserstrasse 15, D-04318 Leipzig, Germany

Correspondence e-mail: hoeche@uni-leipzig.de

Received 9 September 2002
Accepted 20 November 2002

The incommensurately modulated structure of the fresnoite framework-structure type compound $Ba_2TiGe_2O_8$ has been solved using a (3 + 1)-dimensional superspace approach. The structure is orthorhombic and adopts the superspace group $Cmm2(0,\beta,1/2)s00$ with $\beta \simeq 0.635$ at room temperature. The refinement was based on neutron powder diffraction data obtained from a powdered single crystal grown by Czochralski pulling. The modulation parameters that were obtained support the idea that frozen-in rigid-unit modes cause the modulation. The modulation is mainly manifested by positional displacements of O atoms. Barium ions are either eightfold, ninefold or tenfold coordinated in the one-dimensional modulated structure. A significant improvement of the bond-valence sum for both barium positions is achieved by the introduction of the positional modulation. This finding strongly suggests that underbonded barium positions are critically involved in provoking the incommensurate modulation in $Ba_2TiGe_2O_8$.

1. Introduction

In 1965, during geological studies of sanbornit deposits in eastern Fresno County, CA, a new barium silicate mineral was found and named fresnoite, $Ba_2TiSi_2O_8$ (BTS) (Alfors *et al.*, 1965). The crystal structure of BTS comprises corner-connected SiO_4 tetrahedra and TiO_5 square pyramids arranged in sheets that are interspersed with layers of Ba ions (Masse *et al.*, 1967; Moore & Louisnathan, 1969). $Ba_2TiGe_2O_8$ (BTG) was described as isostructural to BTS (Masse & Durif, 1967), and other compounds that adopt or closely resemble the fresnoite framework structure include $Sr_2TiSi_2O_8$ (STS) (Höche *et al.*, 1999, 2002), $Ba_2VSi_2O_8$ (Feltz *et al.*, 1975; Liu & Greedan, 1994), $K_2V_3O_8$ (Galy & Carpy, 1975; Liu & Greedan, 1995), $Rb_2V_3O_8$ (Liu & Greedan, 1995), $Cs_2V_3O_8$ (Andrukaitis *et al.*, 1990) and $(NH_3)_2V_3O_8$ (Liu & Greedan, 1995).

The existence of incommensurate modulations in room-temperature phases of the piezoelectric and pyroelectric fresnoites BTG, BTS and STS has only relatively recently become apparent (Markgraf & Bhalla, 1989; Markgraf *et al.*, 1990; Höche *et al.*, 1999, 2002). The symmetry characterization of these closely related (although not identical) incommensurate structural modulations (superspace-group symmetries, incommensurate primary modulation wavevectors *etc.*) and the structural origin of the various phase transitions in the modulated phases, however, remain somewhat problematic (Halliyal *et al.*, 1985; Iijima *et al.*, 1981; Schmid *et al.*, 1978).

Kimura *et al.* (1973) reported that BTG is modulated at room temperature. The unit cell needed to be doubled along

c_p (where p denotes the parent or average structure) and multiplied by 11 along only one of the two initially equivalent $\langle 110\rangle_p^*$ directions. The structure has orthorhombic rather than tetragonal symmetry. A room-temperature 'average structure' (essentially isomorphous to that of BTS except for a slight orthorhombic strain distortion) was then reported by Iijima *et al.* (1981) (in space group *Cmm*2; $a = 12.31$, $b = 12.292$, $c = 5.366$ Å, *i.e.* $a = a_p - b_p$, $b = a_p + b_p$, $c = c_p$, *cf.* Fig. 1*a*). From the electron-density distribution of this average-structure refinement, it was deduced that the deviation from the parent structure, which causes the additional satellite reflections reported by Kimura *et al.* (1973), had to be associated with the bending of the bridging Ge—O—Ge angles of the Ge_2O_7 pyrogermanate groups, *i.e.* with tetrahedral rotation about c_p. Furthermore, the values of the anisotropic thermal displacement parameters (Iijima *et al.*, 1981) (Fig. 1*b*) clearly indicate that they are very unlikely to merely stem from thermal vibration but might be caused by a positional modulation superimposed over the average structure.

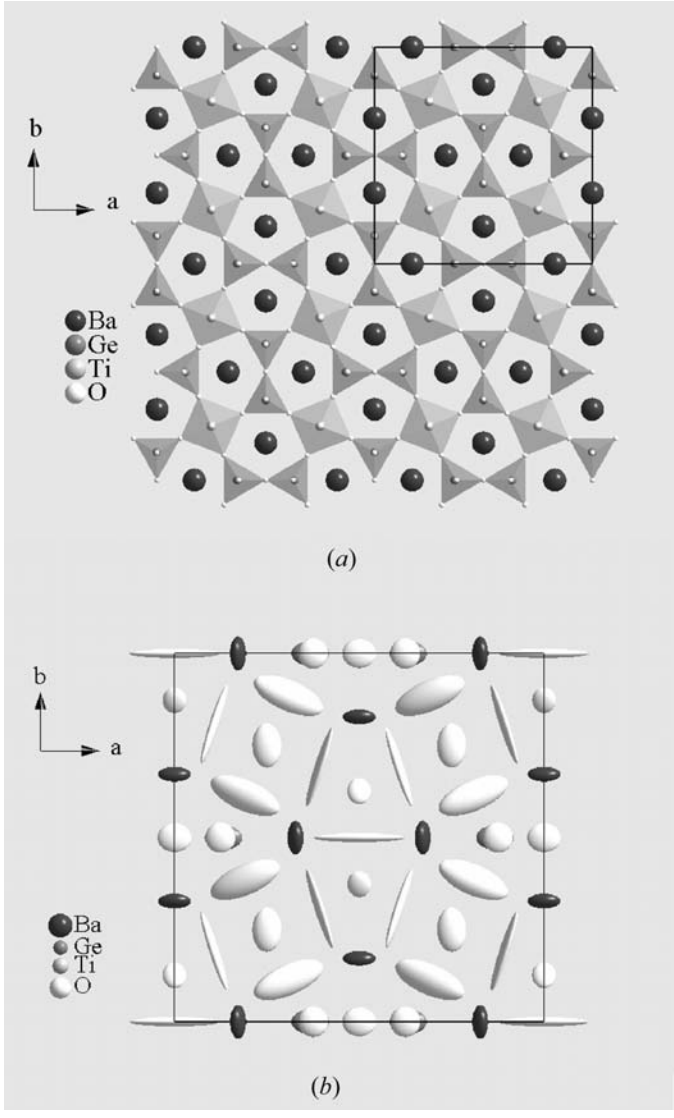

Figure 1
[001] projection of the $Ba_2TiGe_2O_8$ average crystal structure (after Iijima *et al.*, 1981): (*a*) the interconnection of TiO_5 pyramids and Ge_2O_7 pyrogermanate groups underlines the structure of the sheet silicate; (*b*) displacement ellipsoids (95% probability level), particularly of O atoms, were found to be highly anisotropic.

Iijima *et al.* (1981) also reported that a high-temperature phase transition within BTG at 1123 K was improper ferroelastic in character. The satellite reflections of the room-temperature phase are reported to disappear on heating through the transition. Moreover, Markgraf & Bhalla (1989) described an additional low-temperature phase transition (at ~223 K on cooling and ~273 K on heating) that is apparent in dielectric, ultrasonic and pyroelectric measurements. This low-temperature phase transition was proposed to have lock-in transition character with the modulation wavevector magnitude along **a*** locking into a multiple of 1/3.

Most recently, Withers *et al.* (2002) presented a thorough rigid-unit mode (RUM) analysis of the inherent displacive structural flexibility of the ideal fresnoite framework-structure type. Six zero-frequency RUM modes and two close-to-zero-frequency quasi-RUM (q-RUM) modes were found to exist for any modulation wavevector. These RUM modes are all associated with rotations of the constituent SiO_4/GeO_4 tetrahedra and TiO_5 square pyramids around in-plane (*i.e.* perpendicular to **c**) rotation axes. A seventh RUM mode, which involves the rotation of the constituent rigid polyhedra around **c**, was found for the very specific modulation wavevector $\mathbf{q} \sim 0.30\langle 110\rangle_p^*$. The latter RUM mode was identified as playing a major role in the various incommensurately modulated structures observed in $Ba_2TiGe_2O_8$, $Ba_2TiSi_2O_8$ and $Sr_2TiSi_2O_8$.

The current paper presents the superspace-symmetry determination of the incommensurately modulated room-temperature phase of BTG. The structure refinement from neutron powder-diffraction data fully corroborates the hypotheses formulated on the basis of the RUM analysis.

2. Experimental

2.1. Sample preparation

A single-crystalline BTG boule (approximately 60 mm long and 15 mm in diameter) was grown using the automated Czochralski pulling technique with radio-frequency induction heating. Owing to the high melting temperature of this material an iridium crucible had to be used, and therefore the growth was performed under flowing argon. Pulling rates of 0.5 mm h^{-1} and a crystal rotation of 10 min^{-1} were chosen. The axial temperature gradient above the melt was adjusted to *ca* 10 K cm^{-1} by the application of an active afterheater. Because of the lack of a seed, an iridium rod was used for seeding.

2.2. Diffractometry

Neutron single-crystal diffraction experiments were conducted at Studsvik Neutron Research Laboratory in Sweden with a 6 × 6 × 6 mm cube cut off the Czochralski-

pulled BTG single crystal. Since the single crystal was found to host pronounced internal stresses, which were frozen in during the tetragonal-to-orthorhombic phase transition that was passed through during cooling, subsequently neutron powder diffraction was performed at the high-resolution powder diffractometer (HRPD) at ISIS.

For this purpose, the above-mentioned Czochralski-pulled BTG single-crystal cube (*ca* 3 g in weight) was finely ground. HRPD comprises a time-of-flight (TOF) spectrometer with a $\Delta d/d$ resolution of $\sim 4 \times 10^{-4}$, which allows the resolution of lattice-plane spacings down to 0.3 Å. For further processing, TOF data were converted into 2θ data using a home-made computer program by simply applying Bragg's law, $1/d = 2\sin\theta/\lambda$, with a wavelength, λ, fixed to 1.0 Å. This conversion is a simplification of the TOF data, which have rather complex standard deviations and profile functions at different d values. The converted diffraction data that are used in the structure refinement can therefore not fully describe the complex nature of the TOF data. The use of this simplification is believed to be the main reason why the deviation between the experimental and calculated diffractograms is larger at lower 2θ angles ($2\theta < 24.0^\circ$). In the refinement procedure, 2θ values between 26.85 and 27.20° were excluded, since in this range neutrons scattered by the vanadium collimator do contribute to the diffractogram.

The software *JANA*2000 (Petricek & Dusek, 2000) was used for structural refinement of $Ba_2TiGe_2O_8$ with a one-dimensional incommensurate modulation.

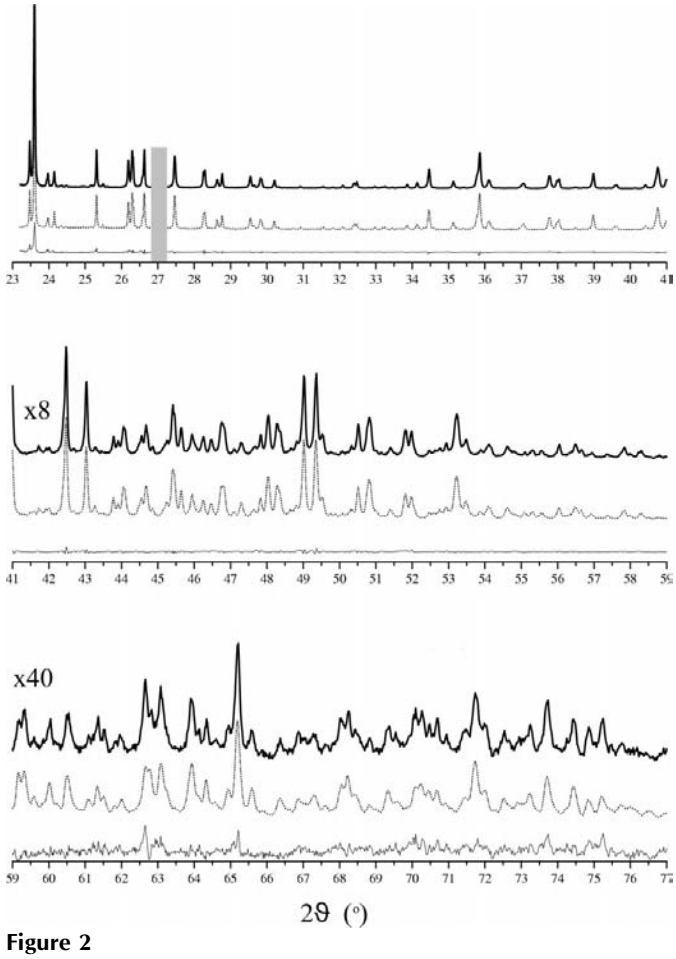

Figure 2
Neutron powder-diffraction data acquired at the HRPD beamline at ISIS (top line), the simulated neutron diffractogram (after refinement of the modulated structure) (middle line), and the difference between theory and experiment (bottom line). Note that the diffraction intensities were multiplied by a factor of 8 between $2\theta = 41$ and 59° and by a factor of 40 between $2\theta = 59$ and 77°. At around $2\theta = 27^\circ$ (within the range indicated by the grey box), intensities stemming from the vanadium collimator were excluded from the refinement.

3. Structure determination

The neutron powder-diffraction data obtained at ISIS are of excellent quality (as illustrated by Fig. 2), particularly at high scattering angles. Owing to the favourable scattering length in the compound studied, satellite reflections are clearly seen above the background (Fig. 3).

The modulated structure of orthorhombic $Ba_2TiGe_2O_8$ was refined in the (3 + 1)-dimensional superspace group $Cmm2(0,\beta,1/2)s00$ with $\beta \simeq 0.635$. The superspace group symmetry was derived from the extinction conditions $F\langle hklm\rangle = 0$ unless $h + k = 2n$ (the *C*-centring) and $l + m = 2n$ [the centring condition in (3 + 1) dimensions] and $F\langle 0klm\rangle = 0$ unless $l = 2n$ (the *s*-glide). Details of the data acquisition and structure refinement parameters of the (3 + 1)-dimensional refinement, which readily converged to $R_{\rm overall} = 0.061$ for a total of 2768 independent reflections (1088 main and 1698 satellites), are compiled in Table 1. Atomic positions and anisotropic displacement parameters are given in the supplementary material,[1] and the displacive modulation wave parameters are listed in Table 2. The background was fitted by eight Chebyshev polynomial coefficients, the peak shapes were modelled using a pseudo-Voigt profile function and the

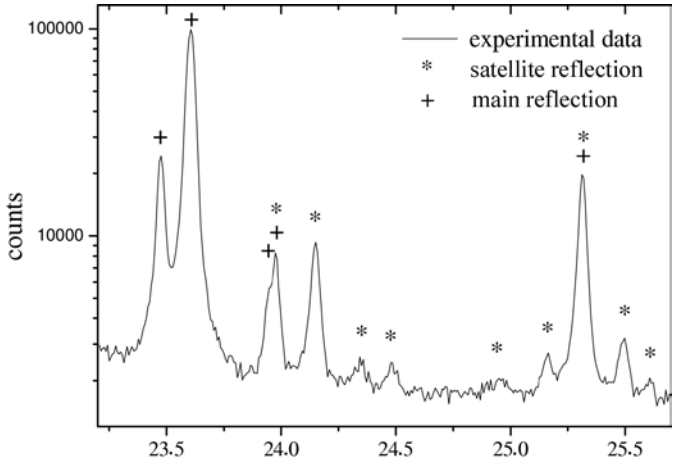

Figure 3
Detail of the experimental neutron powder diffractogram. The satellite reflections (*e.g.* around $2\theta = 24.15^\circ$) are very pronounced and occasionally even clearly separated from the main reflections.

[1] Supplementary data for this paper are available from the IUCr electronic archives (Reference: SN0029). Services for accessing these data are described at the back of the journal.

Table 1
Experimental details.

Crystal data	
Chemical formula	$Ba_2TiGe_2O_8$
Chemical formula weight	595.7
Cell setting, superspace group	Orthorhombic, $Cmm2(0,\beta,1/2)s00$, $\beta \simeq 0.635$
a, b, c (Å)	12.291 (2), 12.274 (2), 10.733 (3)
V (Å^3)	1619.2 (10)
Z	8
Density (g cm^{-3})	4.876
Modulation wavevectors	$\mathbf{q}$ = [0 0.635 0]*†
Crystal form, colour	Finely powdered single crystal, colourless
Powder weight (g)	~3
Data collection	
Diffractometer	HRPD beamline at ISIS
Radiation type	Neutrons
Absorption correction	None
2θ range (°)	23.2–96.9 (26.9–27.2 skipped)
Data collection method	Phi rotation
No. of measured, independent and observed parameters	4294, 4294, 3207
No. of independent and observed satellites	2760, 1978
Criterion for observed reflections	$I \geq 3\sigma(I)$
h, k, l, m range	$0 \leq h \leq 18$ $0 \leq k \leq 19$ $-16 \leq l \leq 16$ $-1 \leq m \leq 1$
Refinement	
R, wR (all reflections)	0.061, 0.049
R, wR (main reflections)	0.056, 0.043
R, wR (first-order satellites)	0.068, 0.058
R, wR (profile)	0.060, 0.059
No. of parameters used in refinement	107
Weighting scheme	$1/I$

† Note that in this sort of situation, it is convention to double the real parent c_p axis to remove the rational component of the primary modulation wavevector (Janssen *et al.*, 1995).

Table 2
Fourier amplitudes of sine (s) and cosine (c) displacive modulation functions.

	Wave	x	y	z
Ba1	s,1	0.0085 (11)	0	0
	c,1	0.0064 (11)	0	0
Ba2	s,1	0	0.0123 (10)	0
	c,1	−0.0066 (9)	0	0.0146 (9)
Ge1	s,1	0.0024 (6)	0	0
	c,1	−0.0121 (6)	0	0
Ge2	s,1	0	0.0107 (5)	0
	c,1	0.0175 (7)	0	−0.0021 (10)
Ti1	s,1	0	0	−0.0070 (14)
	c,1	0.0043 (11)	−0.0204 (12)	0
O1	s,1	0.0142 (5)	−0.0360 (7)	−0.0204 (12)
	c,1	0.0038 (6)	−0.0198 (8)	−0.0008 (15)
O2	s,1	0	0	0
	c,1	−0.0478 (10)	0	0
O3	s,1	0.0256 (6)	0.0195 (5)	−0.0050 (8)
	c,1	0.0173 (6)	−0.0073 (5)	−0.0051 (9)
O4	s,1	0	0	0
	c,1	0.0200 (9)	0	0
O5	s,1	0.0071 (10)	0	0
	c,1	−0.0059 (10)	0	0
O6	s,1	0	0.0115 (10)	0
	c,1	0.0084 (9)	0	−0.0018 (11)
O7	s,1	0	0	−0.0055 (11)
	c,1	0.0024 (12)	−0.0229 (9)	0

asymmetry of the Bragg peaks was modelled with two Berar–Baldinozzi asymmetry parameters.

Only first-order satellites could be observed in the diffraction pattern, which indicates a harmonic type of modulation. A discontinuous modulation, *e.g.* a crenel function, would give higher-order satellites. Therefore, only first-order positional modulation functions were refined.

In order to check the validity of the rigid-unit mode model, a combination of angular and distance constraints (compiled in Table 3) were imposed on the structure during refinement. Under such conditions, the overall R value (main plus satellite reflections) remained at $R_{\rm overall} = 0.100$ ($R_{\rm main} = 0.094$, $R_{\rm satellite} = 0.109$). After releasing the angular restrictions, R values recovered to $R_{\rm overall} = 0.081$, $R_{\rm main} = 0.073$ and $R_{\rm satellite} = 0.092$. This finding proves that GeO_4 tetrahedra and TiO_5 pyramids are not entirely rigid but exhibit a certain degree of flexibility.

4. Discussion

In a recent analysis of rigid-unit modes hosted by the fresnoite framework structure (Withers *et al.*, 2002), the modulated structure in BTG was identified as resulting from the condensation of one of the two initially symmetry-equivalent $\mathbf{q} = \varepsilon\langle 110\rangle_p^* + c_p^*/2$ ($\varepsilon \sim 0.3$) type II RUM modes. Following similar procedures to those set out by Withers *et al.* (2000), an analytical expression for the rotations and shifts of the constituent polyhedra associated with this $\mathbf{q} \sim 0.3\langle 110\rangle_p^*$ zero-frequency RUM mode of distortion was derived independently. After some manipulation this procedure enabled a picture of the resultant RUM displacement pattern to be derived for a condensed $\mathbf{q} = \varepsilon[110]_p^* + c_p^*/2$ mode (Fig. 7 of Withers *et al.*, 2002).

Coefficients of the sine and cosine parts of the modulation waves could be readily obtained from the present analysis of the neutron diffraction data (*cf.* Table 2). Consequently, atomistic representations of the modulated structure for different initial phases of the modulation waves, t, can be easily generated (Figs. 4*a*–4*e*). The striking similarity of our Fig. 4(*a*) and Fig. 7 of Withers *et al.* (2002) impressively illustrates the validity of the approach introduced by Withers *et al.* (2000).

With the information obtained from neutron diffraction data, a very instructive representation of the modulated structure of BTG can be obtained, where approximants of the structure are plotted for closely spaced t values. Fig. 4 shows a series of five approximants for $t = 0, \ldots, 0.2$ ($\Delta t = 0.05$), and an even more illustrative Pack & Go PowerPoint presentation is given in the supplementary material. Series of approximants with increasing t can be interpreted in two ways. Firstly, they represent the modulated structure at different loci within the BTG crystal, and secondly, they can be regarded as time-dependent snapshots of the ideal *P4bm* parent BTG structure characterized at temperatures above the non-modulated-to-

modulated phase transition by dynamically excited rigid-unit modes.

As proved by the introduction of bond-length and bond-angle constraints into the refinement, a significant distortion of the TiO_5 and GeO_4 polyhedra is superimposed on these dynamically excited RUMs. In Fig. 5, O—Ge1—O and O—Ge2—O bond angles are plotted *versus t*; compared with actual bond-angle values of the non-modulated structure, deviations of up to about 6° can be discerned. The average values for $(Ge1)O_4$ and $(Ge2)O_4$ tetrahedra, however, differ by less than 0.05% and are generally very close to the ideal value of 109.47° for a regular tetrahedron. Within the GeO_4 tetrahedra, bond lengths are virtually not affected by the modulation and in TiO_5 pyramids bond-length changes and O—Ti—O bond-angle distortions are within experimental uncertainties. In fact, TiO_5 pyramids essentially rotate about

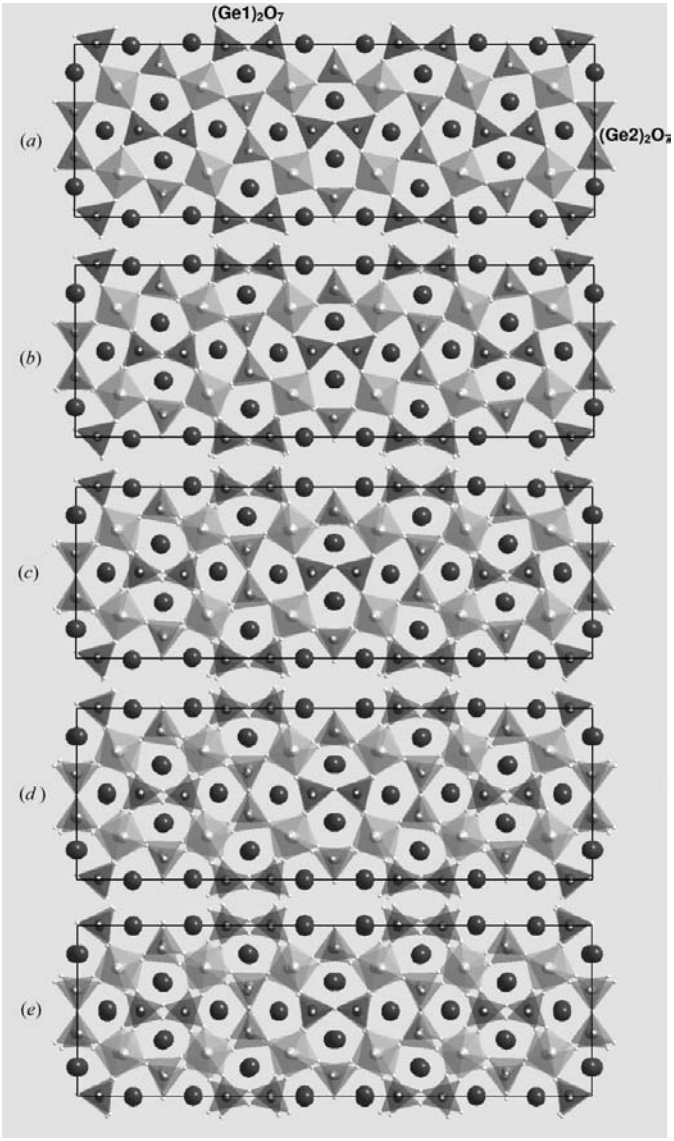

Figure 4
Series of $1 \times 3 \times 2$ approximants of the incommensurately modulated BTG structure in projection along [001]: (*a*) $t = 0.01$, (*b*) $t = 0.05$, (*c*) $t = 0.1$, (*d*) $t = 0.15$, (*e*) $t = 0.2$. For $t = 0.25$ to $t = 0.45$, the series is reiterated in the opposite order [from *a* to *e* and the whole series ($t = 0.0$ to $t = 0.45$), *i.e.* *a* to *e* to *a*] is repeated once again between $t = 0.5$ and $t = 0.95$. A much clearer presentation is given in the supplementary material.

Table 3
Constraints (°, Å) imposed on the modulated BTG structure during refinement to test the validity of the rigid-unit mode model.

Constraint	Value
O6—Ge2—O4	109.4
O3—Ge2—O4	109.4
O3—Ge2—O6	109.4
O1—Ge1—O2	109.4
O5—Ge1—O2	109.4
O5—Ge1—O1	109.4
Ge1—O5	1.70
Ge1—O2	1.70
Ge1—O1	1.70
Ge2—O4	1.70
Ge2—O3	1.70
Ge2—O6	1.70
Ti1—O1	1.90
Ti1—O3	1.90
Ti1—O7	1.73

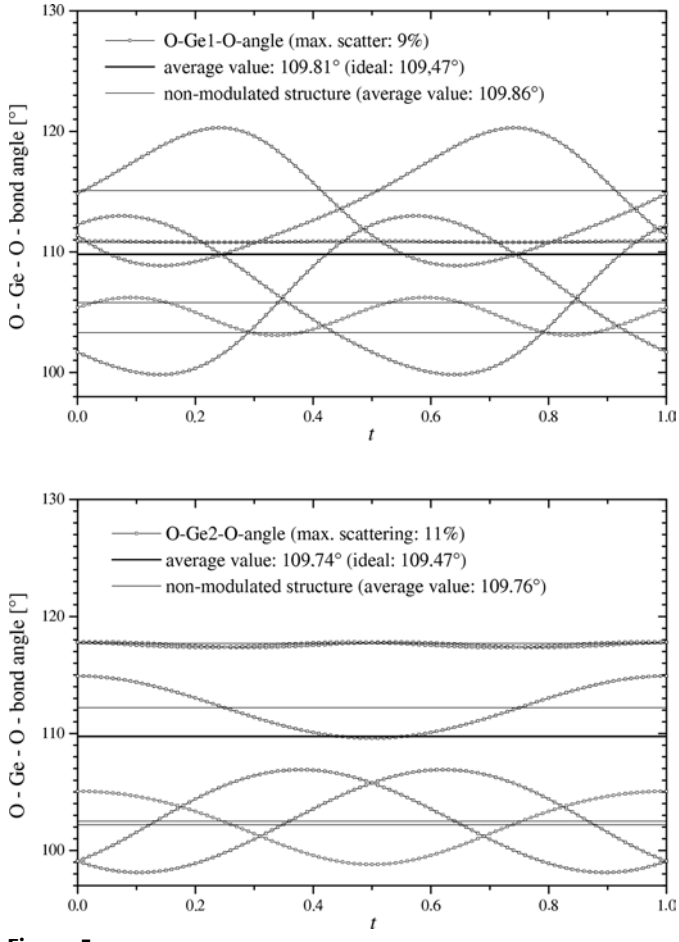

Figure 5
Dependence of O—Ge—O bond angles on the initial phase of the modulation waves, *t*: (*a*) Ge1 sites and (*b*) Ge2 sites. For comparison, bond angles measured in the non-modulated structure and the main value for the modulated structure (average over all O—Ge—O angles and all *t* values) are given.

their c axes and it is found that TiO_5 pyramids belonging to subsequent layers move slightly off phase, like a coupled pendulum.

Returning to Figs. 4(*a*)–4(*e*), it can be clearly seen that along the c axis upper and lower sheets are distorted about barium sites in antiphase. Moreover, the sets of two pentagonal rings encircling different barium sites are found to be more (Ba2) or less (Ba1) symmetric. Consequently, on average, t-dependent bond-valence sums (Brese & O'Keeffe, 1991) are more favourable for Ba2 (Fig. 6). In the non-modulated structure, Ba2 has a very unsatisfactory bond-valence sum of only 1.70. With the introduction of the positional modulation, on average, the bond-valence sum can be very much improved to 1.95. Similarly, the bond-valence sum of Ba1 is improved from 1.81 (non-modulated structure) to 1.88. These results support the idea that the modulation is provoked by significantly underbonded large cations in the fresnoite framework structure. This hypothesis was initially established for melilites (*e.g.* Seifert *et al.*, 1987) and more recently extended to the fresnoites during structural studies at $Sr_2TiSi_2O_8$ (Höche *et al.*, 2002). $Ba_2TiGe_2O_8$ is similar to $Sr_2TiSi_2O_8$ in that the bond-valence sums for titanium and germanium are close to their optimum values, irrespective of whether modulation waves are introduced or not.

As changes in the bond-valence sums are caused by changes in bond length, the t dependence of the Ba—O distances is worth considering. Since barium ions are usually coordinated with eight or more oxygen ions, Ba—O bond lengths are generally rather large. In the fresnoite framework structure, barium is said to be tenfold coordinated. This fact implies that barium and oxygen ions further apart than 3.5 Å should not be considered as bonded since, in the non-modulated average structure, Ba—O bond lengths (*cf.* Table 4) do not exceed 3.5 Å. Plotting the interatomic distances, d, between Ba1 and the surrounding oxygen ions (Fig. 7*a*), and the distances between Ba2 and the associated oxygen-ion positions (Fig. 7*b*) for the modulated structure against t reveals coordination changes across the modulated crystal. With the definition introduced above, Ba1 is eightfold coordinated for $t = 0$, ninefold coordinated for $t = 0.16$ and tenfold coordinated for $t = 0.4$. Averaging over t, a coordination number of 9.0 for Ba1

Table 4
Ba—O bond lengths measured in the average structure.

Crystallographic sites	Bond distance (Å)	Degeneracy
Ba1—O3	2.672 (6)	1×
Ba1—O6	2.812 (12)	2×
Ba1—O5	2.814 (15)	1×
Ba1—O1	2.886 (21)	2×
Ba1—O4	3.081 (25)	2×
Ba1—O7	3.428 (6)	2×
Ba2—O6	2.704 (18)	1×
Ba2—O3	2.818 (10)	2×
Ba2—O4	2.870 (23)	2×
Ba2—O2	2.890 (27)	1×
Ba2—O1	3.167 (24)	2×
Ba2—O7	3.423 (6)	2×

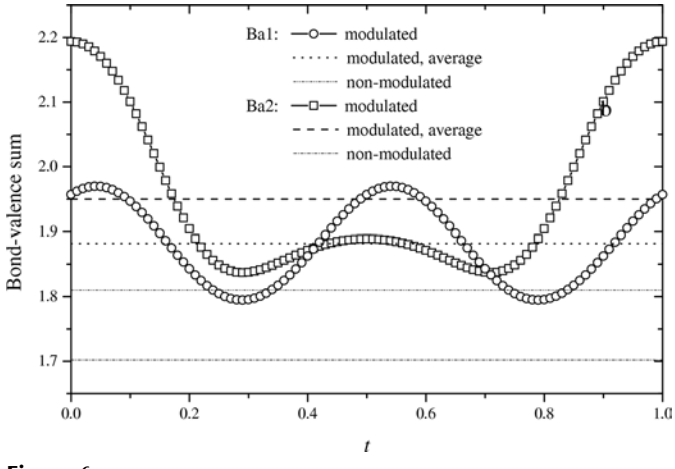

Figure 6
t-dependence of bond-valence sums for Ba1 and Ba2 positions in the modulated BTG structure. Values averaged over t and without modulation waves are also plotted. For bond-valence calculations within the non-modulated structure, a cut-off radius of 3.5 Å was used, while in the modulated structure, a cut-off at 3.2 Å was employed.

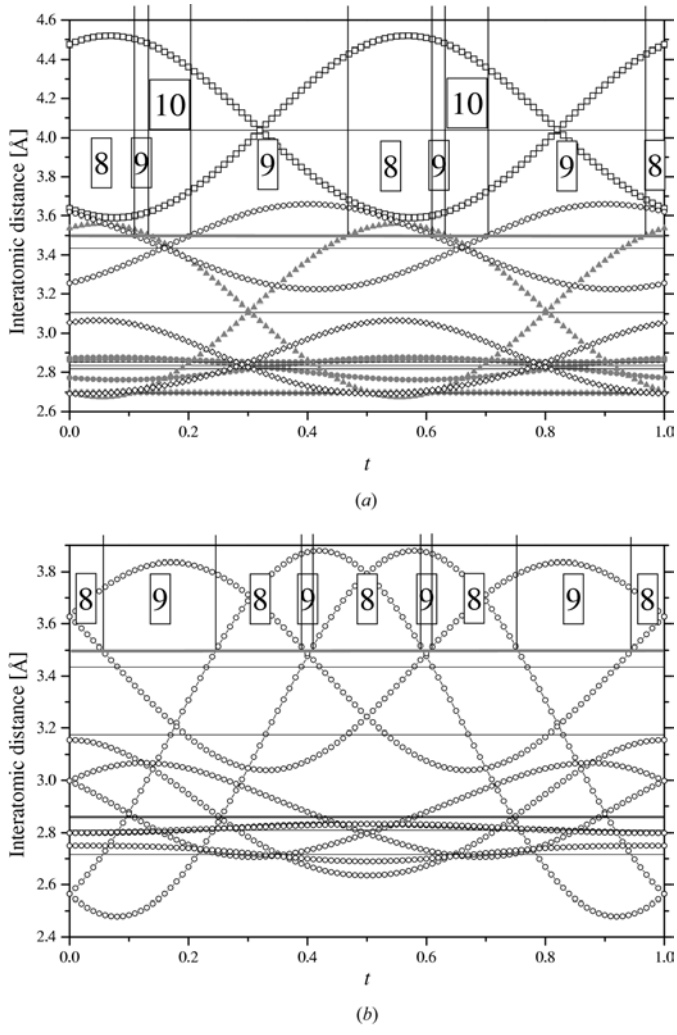

Figure 7
Ba—O bond length as a function of t. Coordination numbers of barium ions based on the 3.5 Å limit are given in the plot in boxes: (*a*) Ba1—O distances and (*b*) Ba2—O distances. Greater distances are not shown.

is found. Setting the bond-length limit slightly higher (3.6 Å) even results in an elevenfold coordination close to $t = 0.7$ and 0.57, since two atoms that are more than 4 Å apart in the average structure will approach Ba1. A similar scattering of local coordination numbers has been reported by Bindi *et al.* (2001) for the large cation in a natural melilite (Bindi *et al.*, 2001). In the Ba1—O *d-versus-t* plot, the average distances of initially identically spaced species are preserved (*e.g.* two atoms at a distance of 4.03 Å from Ba1 in the average structure simultaneously get closer to/further away from Ba1 by the same amount). This symmetry about lines of constant *d* is not found in the *d-versus-t* plot for Ba2. Here, degenerate distances resolve into branches that are symmetric about lines of constant *t*. Within the 3.5 Å limit the coordination number for Ba2 is always between 8 and 9; the average value is 8.4.

In agreement with findings reported by Bindi *et al.* (2001) for *X* and O3 sites in the closely related $X_2T1(T2)_2O_7$ melilite structure, strong residual electron densities in the neighbourhood of the actual modulated positions of Ba1, Ba2 and O3 sites in $Ba_2TiGe_2O_8$ do exist. Therefore, modulations of the thermal parameters were introduced. *R* values decreased from 0.056 to 0.041 (main reflections) and 0.068 to 0.053 (satellites), respectively. However, the refinement quickly became unstable, which indicates that the information contained in the powder-diffraction data is not detailed enough to support such refinements. In conclusion, the occurrence of thermal-displacement parameter modulations in BTG is very likely, but because of the lack of single-crystal neutron diffraction data (highly-strained crystal) this modulation cannot be further investigated.

Figs. 4(*a*)–4(*e*) further show that there are two clearly distinct pyrogermanat groups. While the $(Ge1)_2O_7$ groups easily skew (in antiphase with the neighbouring group one sheet layer above or below), the $(Ge2)_2O_7$ groups merely rotate rigidly about the bridging oxygen ion located at their centre of mass (the corresponding group in the neighbouring sheets rotates slightly out of phase). Based on these findings, a hypothesis concerning the structural changes associated with replacing germanium sites in BTG by silicon can be posed. Schmid *et al.* (1978) reported on the complete miscibility of $Ba_2TiGe_2O_8$ and $Ba_2TiSi_2O_8$ and pointed out that the space group of the mixed crystal changes at a 1:1 ratio of silicon and germanium (*Cmm*2 on the germanium-rich side and *Pb*4*m* on the silicon-rich side). Taking into consideration the higher stiffness of the O—Si—O bond, it is reasonable to assume that silicon can be incorporated until all Ge2 sites are replaced by silicon, and any further increase in the silicon content will disturb the inherent flexibility of the BTG structure and cause a change in the crystal symmetry. Currently, a $Ba_2TiSiGeO_8$ sample is under investigation in order to check the validity of the suggested mechanism.

Although *t*-dependent trajectories of oxygen-ion positions reproduce precisely the shape of displacement ellipsoids, the latter are still slightly anisotropic after considering the modulated structure (Fig. 8). This might be indicative of the subsequent lower-temperature phase transformation described by Markgraf & Bhalla (1989), which might, according to Withers *et al.* (2002), be associated with the condensation of a still not-frozen-in RUM mode.

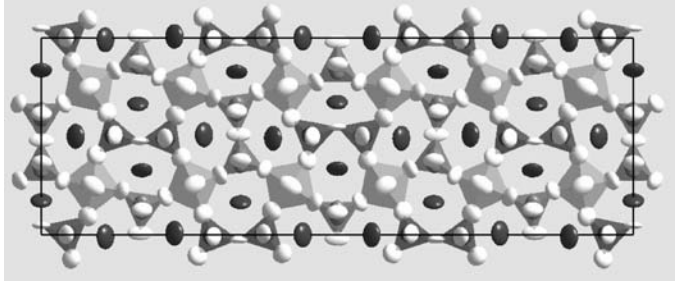

Figure 8
Displacement ellipsoids on the 95% probability level superimposed on the $1 \times 3 \times 2$ approximant of the modulated BTG structure for $t = 0.01$.

Valuable discussions with Dr Jekabs Grins and Dr Vaclav Petricek are gratefully acknowledged. The authors thank Dr Kevin Knight at ISIS for NPD data collection. SE thanks the Blanceflor foundation for financial support. TH and WN acknowledge financial support provided by Deutsche Forschungsgemeinschaft (contracts NE 646/8–1, RU 417/6–1).

References

Alfors, J. T., Stinton, M. C., Matthews, R. A. & Pabst, A. (1965). *Am. Mineral.* **50**, 314–340.
Andrukaitis, E., Jacobs, P. W. M. & Lorimer, J. W. (1990). *Can. J. Chem.* **68**, 1283.
Bindi, L., Bonazzi, P., Dusek, M., Petricek, V. & Chapuis, G. (2001). *Acta Cryst.* B**57**, 739–746.
Brese, N. E. & O'Keeffe, M. (1991). *Acta Cryst.* B**47**, 192–197.
Feltz, A., Schmalfuss, S., Langbein, H. & Tietz, M. (1975). *Z. Anorg. Allg. Chem.* **417**, 125–129.
Galy, J. & Carpy, A. (1975). *Acta Cryst.* B**31**, 1794–1795.
Halliyal, A., Bhalla, A. S., Markgraf, S. A., Cross, L. E. & Newnham, R. E. (1985). *Ferroelectrics*, **62**, 27–38.
Höche, T., Neumann, W., Esmaeilzadeh, S., Uecker, R., Lentzen, M. & Rüssel, C. (2002). *J. Solid State Chem.* **166**, 15–23.
Höche, T., Rüssel, C. & Neumann, W. (1999). *Solid State Commun.* **110**, 651–656.
Iijima, K., Marumo, F., Kimura, M. & Kawamura, T. (1981). *J. Chem. Soc. Jpn*, **10**, 1557–1563.
Janssen, T., Janner, A., Looijenga-Vos, A. & de Wolff, P. M. (1995). *International Tables for Crystallography*, edited by A. J. C. Wilson, Vol. C, pp. 797–844. Dordrecht: Kluwer Academic Publishers.
Kimura, M., Doi, K., Nanamatsu, S. & Kawamura, T. (1973). *Appl. Phys. Lett.* **23**, 531–532.
Liu, G. & Greedan, J. E. (1994). *J. Solid State Chem.* **108**, 267–274.
Liu, G. & Greedan, J. E. (1995). *J. Solid State Chem.* **114**, 499–505.
Markgraf, S. A. & Bhalla, A. (1989). *Phase Transit.* **18**, 55–76.
Markgraf, S. A., Randall, C. A., Bhalla, A. & Reeder, R. J. (1990). *Solid State Commun.* **75**, 821–824.
Masse, R. & Durif, A. (1967). *Bull. Mineral.* **90**, 407–408.
Masse, R., Grenier, J.-C. & Durif, A. (1967). *Bull. Soc. Fr. Mineral. Cristallogr.* **90**, 20–23.
Moore, P. B. & Louisnathan, S. J. (1969). *Z. Kristallogr.* **130**, 438–448.
Petricek, V. & Dusek, M. (2000). *JANA*2000. Institute of Physics, Praha, Czech Republic.

Schmid, H., Genequand, P., Tippmann, H., Pouilly, G. & Guedu, H. (1978). *J. Mater. Sci.* **13**, 2257–2265.
Seifert, F., Czank, M., Simons, B. & Schmahl, W. (1987). *Phys. Chem. Miner.* **14**, 26–35.
Withers, R. L., Tabira, Y., Liu, Y. & Höche, T. (2002). *Phys. Chem. Miner.* **29**, 624–632.
Withers, R. L., Tabira, Y., Valgoma, J. A., Arroyo, M. & Dove, M. T. (2000). *Phys. Chem. Miner.* **27**, 747–756.